Electrodiffusion active pump model with asymmetric immersed chemical potentials

Pilhwa Lee[a,1]

This manuscript was compiled on December 6, 2025

Electrodiffusion is essential in understanding the mechanisms of electrophysiology. Regarding volume homeostasis, active exchange pumps are critical, as is also significant in the mechanisms of cell division, growth, and apoptosis. In the sense of the immersed boundary (IB) method, we replace classical interface conditions across the membrane with regularized chemical potentials to control the permeation of each ionic species governed by the Poisson-Nernst-Planck equation. As a consequence of the model simulation, electroneutrality, except for the thin space charge layers along the membrane, is well satisfied. In asymmetry, to regulate ionic transport, continuous chemical potential barriers are augmented with energetic gradients represented by smoothed Heaviside kernels specifying the directions of active pumps. We obtain steady-state concentrations from electrodiffusion active pumps with Na^+, $^K+$, Cl^- ionic species and background charges in the unified entire domain with periodic boundary conditions. The electrodiffusion active pump model for the exchange of sodium and potassium (NKE) exhibits a good fit to the theoretical formula over a broad range of perturbations in ionic concentrations, ensuring volume conservation in the steady state only when active pumps are functioning. It is also shown that van't Hoff's law is satisfied without active pumps. This is a foundation for applying the IB electrodiffusion active pump model for subcellular transport of water and molecules, possibly involving cell motility and migration.

Electrodiffusion | active transport | the immersed boundary method

Significance Statement

Active pumps are crucial for cellular homeostasis, keeping physiological states. The new computational model for active pump resolves sharply thin space charge layers around membranes in a non-asymptotic manner without the assumption of homogeneous local and global electroneutrality in electrodiffusion. The microscopic representation of kinetic interaction between the water semi-permeable membrane and solutes mediated by the prescribed continuous chemical potential barriers through fluctuation-dissipation satisfies the macroscopic osmotic balance, i.e. van't Hoff law, when there are no active pumps. The biophysical model shows the expected homeostatic volume regulation with active pumps and swelling phenomena without their working. The model framework is applicable to rigorously characterize physiological and disease states involving the coupled electrical and osmotic effects with possible membrane movement.

Brownian ratchet with asymmetric potential walls represents active chemical potential with ATP hydrolysis (1, 2). As one specific mode of microscopic machineries of directed transport with ATP hydrolysis, for example, rotary protein motors utilize chemical potentials with ATPase (3, 4). In this article, we introduce asymmetric chemical potentials to represent passive and active transport in the superposition of regularized singular integrals of Dirac delta and Heaviside kernels.

Cell membranes are water-permeable, but many macromolecules (e.g., sugar) are not permeable across the membrane (5). By this water semi-permeable property of the membrane, we observe diverse osmotic effects, osmosis. For instance, the water transport in the epithelial cell (6), the osmotic power in MEMS (7), the DNA packaging in the vesicle (8), and the osmophoresis (9, 10) are all involved with them. Regarding volume homeostasis, in the presence of a non-uniform distribution of concentration between intracellular and extracellular domains and highly concentrated negatively charged macromolecules inside (e.g., proteins, nucleic acids), without elasticity of the plasma membrane and exchange pumps working together, the cell inevitably swells (11–13); the volume swelling of a dead cell is a good example. Active exchange pumps involved in cellular volume regulation are also significant in the mechanism of cell division, growth, and apoptosis (14).

In electrodiffusion in subcellular scales, along the plasma membrane, the assumption of electroneutrality is not satisfied. There come the electrical double layers, so-called the *Debye layer* or *space charge layer*. In physiological ionic concentrations, the thickness of the space charge layers is around 10 nm. This is deeply involved in electro-osmosis and active ion pumps for cell migration (10, 15), even though these studies do not represent the space charge layers in finite dimensions. Electrokinetic phenomena, the hydrodynamics of electrolytes driven by an electrical field, are all related to this mechanism, and they are significant in the flow or particle control in micro and nanofluidics. The related primary physical structure is again the *Debye layer* generated at the interface between fluid and dielectric or conducting structure as described by (16). The accompanying migration of a structure immersed in fluids is called electrophoresis. The electrophoresis has been applied to protein and molecule separation by capillary

Author affiliations: [a]Department of Mathematics, Morgan State University

[1]To whom correspondence should be addressed. E-mail: Pilhwa.Lee@morgan.edu

DRAFT

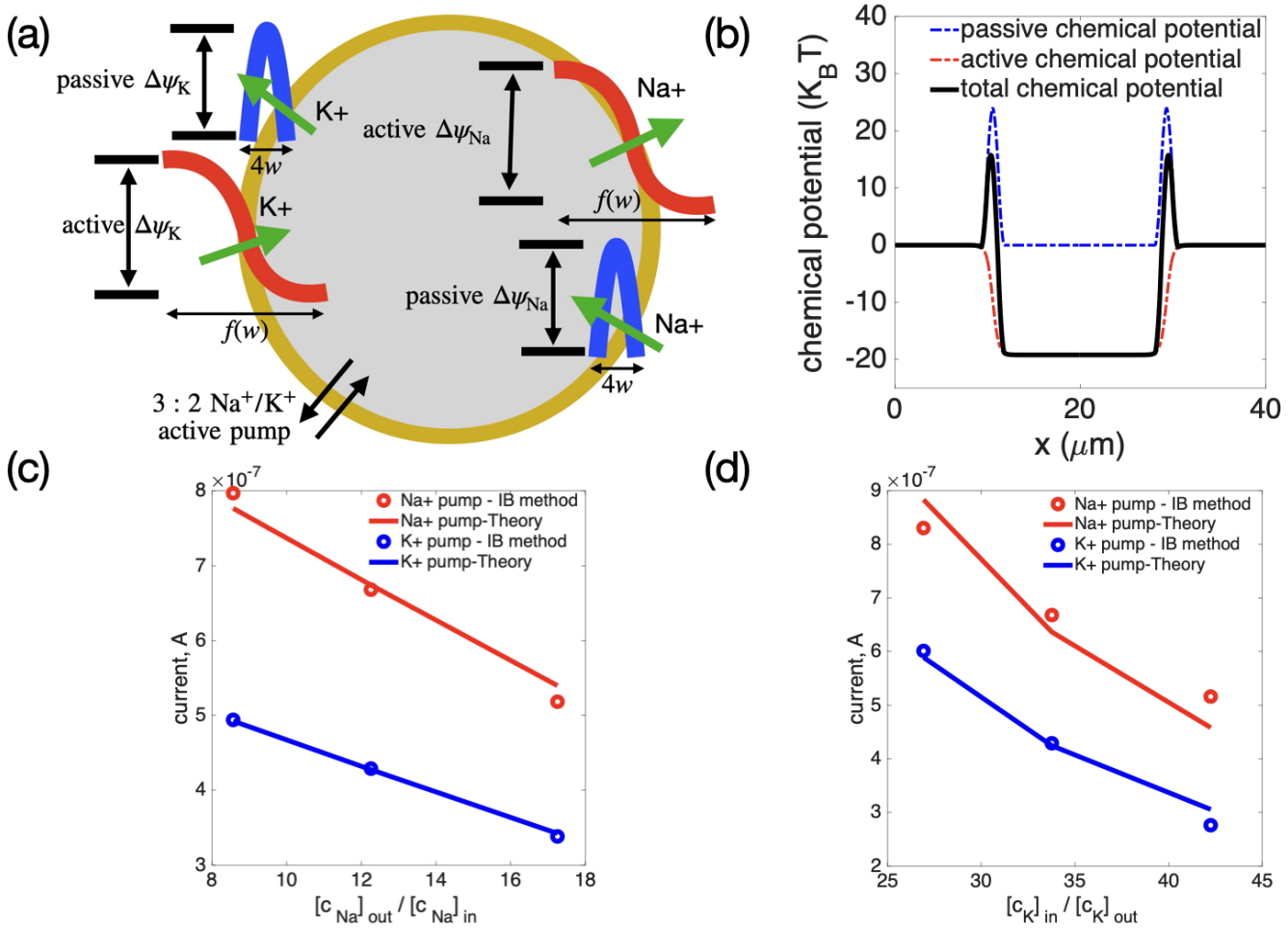

Fig. 1. (a) Schematic representation of the active pump model with asymmetric chemical potentials. (b) Chemical potential distributions for active pumps (red dotted profile, smoothed Heaviside), passive membrane permeation (blue dotted profile, smoothed Dirac delta function), and superposition of active and passive transmembrane transport (black solid profile). (c) and (d) The fluxes of NKE pump, outflux of sodium ions (red circles) and influx of potassium ions (blue circles) computed from the immersed boundary (IB) method, are compared with the theoretical formula (SI Eq. 10), solid curves) with variation in the ratio of $[\mathrm{Na}^+]_{\mathrm{out}}/[\mathrm{Na}^+]_{\mathrm{in}}$ and $[\mathrm{K}^+]_{\mathrm{in}}/[\mathrm{K}^+]_{\mathrm{out}}$.

electrophoresis, as shown in (17, 18), and diagnostics described in (19). In the context of proteomics on a chip, the details are referred to (20, 21). The biological cell also implements active pumping mechanisms for spontaneously generated electric fields and induced migration (22). The concentration gradient generated from external electric fields and space charge layers induces electrophoresis coupled with osmotic effects. The mobility of the vesicle is enhanced by more than 100% in the case of water semi-permeable vesicles (23).

Osmotic effects have been modeled with chemical potential barriers (24–26). In the formalism of the immersed boundary method (27–29), which is mathematical and computational framework for fluid-structure interaction (30), chemical potential barriers are applied for the drift-diffusion of solutes or electrically charged ions, realizing their mediation of osmotic effects.

Active pump models have been approached in macroscopic points of view (31–34), and specifically for cellular volume regulation and water transport (35–38). Within the macroscopic pump-leak models, electrodiffusion was addressed by (39, 40), but prescribing electroneutrality uniformly even in the space charge layers. There is one approach where surface charge layers are represented in the electroneutral asymptotic limit of electrodiffusion with its well-posedness (41).

In experiments, surface charge layers were shown to be significant with the involving phospho-lipids for closing feedback loop in cellular protrusion, polarity, and migration (42). Indeed, cell polarity is involved with $\mathrm{Na}^+/\mathrm{H}^+$ exchange pumps (43). Most ion channels use surface charges to increase the rates of ionic entrance (44).

The present article focuses on the electrodiffusion active pump model with the immersed chemical potentials, in the sense of the IB method. The prescribed immersed chemical potentials represent both passive permeation and active pumping. With the presence of regularized bell-shaped chemical potential barriers, the passive ionic transport does exist. Concurrently, regularized Heaviside chemical potentials work as directed active pumps. Still, overall, there

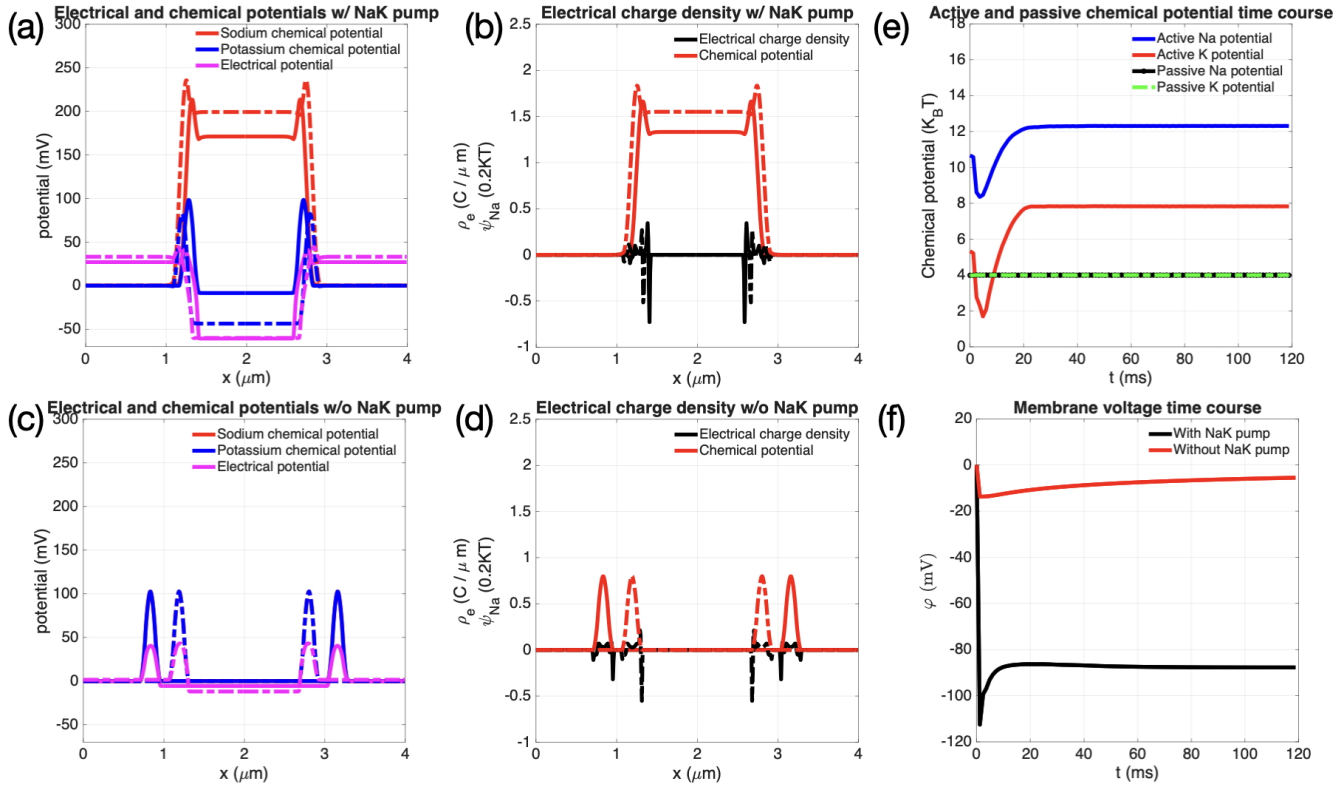

Fig. 2. Electrical and chemical potential distributions and time courses. (a) and (c) Electrical and chemical potential distributions with and without the NKE pump. (b) and (d) Electrical charge density distribution with and without NKE pump. Solid curves and dotted curves are for t=120ms and t=6ms. (e) Active components of the chemical potentials for sodium (blue) and potassium (red) ionic species. Passive components of the chemical potentials for sodium (black) and potassium (green) are represented by dotted curves. (f) Membrane potential time courses with and without NKE pump.

comes a non-equilibrium steady state with the proposed model. We have observed macroscopic van Hoff's law from microscopic kinetic interaction among semi-permeable membranes and solutes via immersed chemical potentials in the sense of fluctuation-dissipation without active pumps. The cases of membranes as free boundaries floating with and without active pumps are mainly explored in the main article, and the cases of fixed boundaries are supplemented in the Appendix. The proposed model does demonstrate active pumping essential for cellular volume conservation while *capturing the finite dimension of the space charge layers along the membrane.*

1. Model description

A. The chemical potentials for active and passive transports. The passive membrane permeation is represented by chemical potentials via a smoothed Dirac delta function (Figure 1(b), blue dotted profile). Active pumps are represented by chemical potentials with smoothed Heaviside functions (Figure 1(b), red dotted profile). The overall chemical potentials are constructed in a superposition of active and passive transmembrane transport (black solid profile). The detailed formulation is in the SI.

B. Active transport model formulation with current to potential map. In order to represent the active transport, the chemical potential is prescribed with its amplitude across the immersed boundaries in the following:

$$A_i^{\text{active}} = A_i \cdot (1 + a_{i,0} \cdot \log(J_{\text{current}}^{\text{potential}} \cdot a_{i,1})). \quad [1]$$

where the specific parameter values are in SI Table 2. Here, the current to potential map, $J_{\text{current}}^{\text{potential}}$ does represent the main formulation of transmembrane current kernel in terms of ionic concentrations and membrane potentials applied to construct the chemical potential amplitudes A_i^{active} for active pumping of ith ionic species.

C. Free boundaries as immersed chemical potential barriers interacting with elastic membranes. The one-dimensional membranes of X_a and X_b represent the cross-section of the cell. The cellular elastic tension at the membranes X_{a} and X_{b} is transmitted to the solutes/ions and fluid as F_{ms} and F_{mf}, respectively in the sense of fluctuation and dissipation. For example, for the left membrane at the Lagrangian coordinate X_{a},

$$F_{\text{ms}}(X_{\text{a}}) + F_{\text{mf}}(X_{\text{a}}) = -K(X_{\text{b}} - X_{\text{a}} - L), \quad [2]$$

where L is the resting length at $t = 0$, and K is the elastic stiffness. From the principle that the total integral of Eulerian chemical force densities from each ionic species with respect to X is the same as the Lagrangian force at X in the Eulerian domain of Ω_{E}, as an arbitrarily defined local neighborhood of X:

$$F_{\text{ms}}(X) = \int_{\Omega_{\text{E}}} \sum_k -\nabla\psi_k(x - X)c_k(x)dx, \quad [3]$$

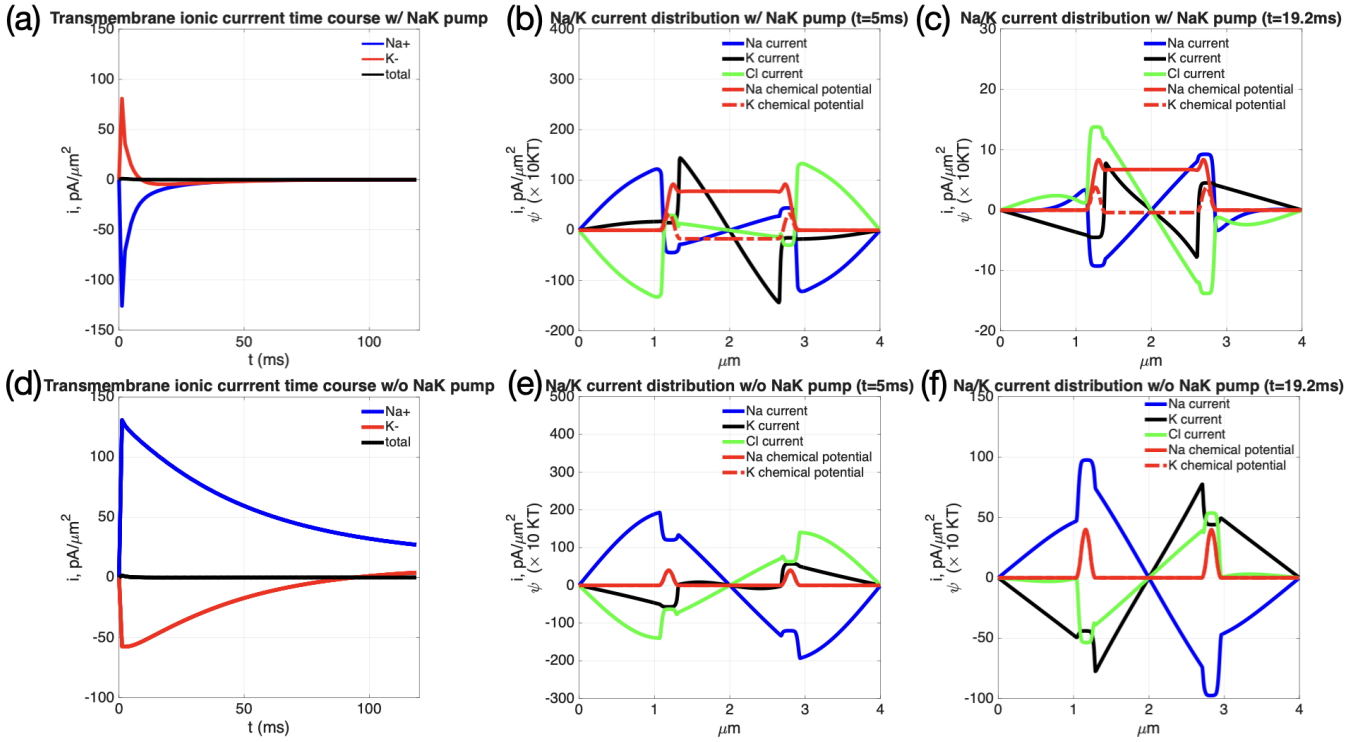

Fig. 3. Ionic current distributions and time courses (a) and (d) Transmembrane Ionic currents and total current time courses with and without NKE pump. (b) and (e) Ionic current distributions with and without NKE pump at t=5.0ms. (c) and (f) Ionic current distributions with and without NKE pump at t=19.2ms. Chemical potentials for sodium and potassium ionic species are also shown in red solid and dotted profiles.

and F_{mf} can be explicitly formulated as follows:

$$F_{\mathrm{mf}}(X_{\mathrm{a}}) = -K(X_{\mathrm{b}} - X_{\mathrm{a}} - L) + \int_{\Omega_{\mathrm{E}}} \sum_k \nabla\psi_k(x - X_{\mathrm{a}})c_k(x)dx. \quad [4]$$

In the Stokes flow in the 1D domain, the fluid flow is just stationary ($u = 0$). Accordingly, the relative sliding between the semi-permeable membrane and fluid, and the associated drag is induced by F_{mf} in the following:

$$\zeta\frac{\partial X}{\partial t} = F_{\mathrm{mf}} \cdot N, \quad [5]$$

where N is the unit vector indicating the outer normal direction, and ζ is the osmotic stiffness.

2. Results and Discussion

A. NKE model construction. The current to potential map for the sodium-potassium active pump is prescribed in the following based on the theoretical formulation of active exchange fluxes (SI Eq. 10):

$$J_{\mathrm{current}}^{\mathrm{potential}} = \frac{G_{\mathrm{V,NKE}}}{(1+\beta_{\mathrm{NKE,Na}}\Gamma_{\mathrm{Na}})^3(1+\beta_{\mathrm{NKE,K}}/\Gamma_{\mathrm{K}})^3}. \quad [6]$$

The results with fixed boundaries from the IB method with the immersed chemical potentials (solid curves) are fitted with the theoretical formula of the flux terms of the Na^+/K^+ active pump (NKE) (Fig. 1(c) and (d)), i.e., outflux of sodium ions (red circles) and influx of potassium ions (blue circles) with variations in the ratios of $\Gamma_{\mathrm{Na}} = [\mathrm{Na}^+]_{\mathrm{out}}/[\mathrm{Na}^+]_{\mathrm{in}}$ and $\Gamma_{\mathrm{K}} = [\mathrm{K}^+]_{\mathrm{in}}/[\mathrm{K}^+]_{\mathrm{out}}$ in the initial configuration of ionic concentrations.

B. Ionic distributions associated with the chemical potentials. The electrodiffusion active pump model is simulated with free membranes. The ionic distributions are shown to be adjusted with the moving boundaries in Figure S2. For comparison, the active pump is turned off and a moderate amount of sodium and potassium ions are flooded in and out of the membranes. Figure S2 shows sodium ionic distribution with and without NKE (panel (a) and panel (d)), potassium ionic distribution with and without NKE (panel (b) and panel (e)), chloride ionic distribution with and without NKE (panel (c) and panel (f)). Solid and dotted black profiles are for the distribution at the steady state of t=120ms and at the initial t=0ms. Red profiles are for chemical potential distributions.

C. Electrical and chemical potential distributions and time courses. The electrical potentials and electrical charge densities are shown with free boundaries in Figure 2 with and without active pumps. Electrical and chemical potential distributions are shown with and without NKE (Panel (a) and Panel (c)), electrical charge density distribution with and without NKE (Panel (b) and Panel (d)). Solid curves and dotted curves are for t=120ms and t=6ms. Active components of the chemical potentials are represented by solid curves for sodium (blue) and potassium (red) ionic species. Passive components of the chemical potentials for sodium (black) and potassium (green) are represented by dotted curves (Panel (e)). Membrane potential time courses are shown with and without NKE (Panel (f)). Resting membrane potential is recapitulated around -80mV with the active pump. Without an active pump, the membrane is tonically depolarized unsteadily. The proposed electrodiffusion model

DRAFT

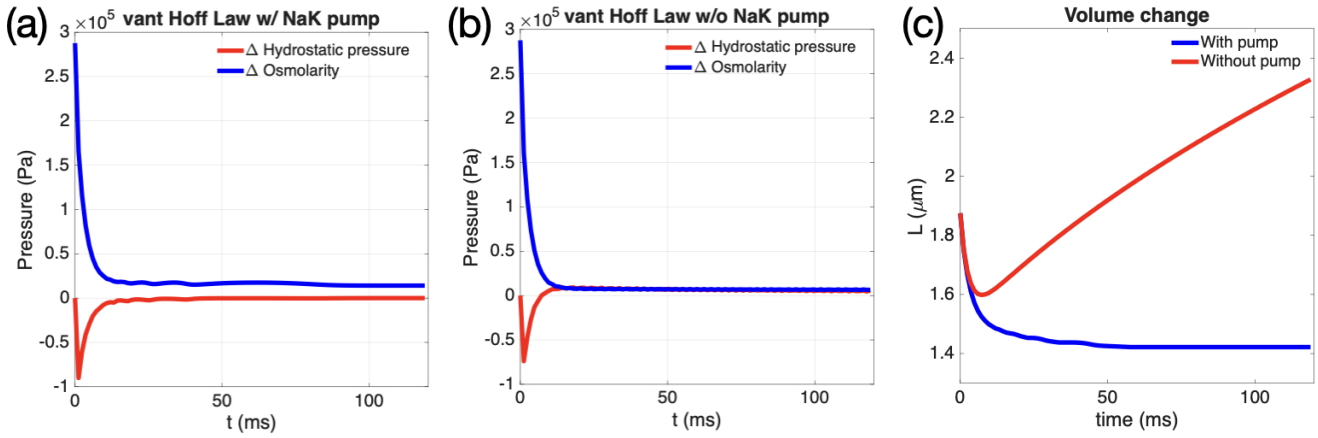

Fig. 4. Hydrodynamic pressure versus osmotic pressure. (a) and (b) Time course of pressure and osmolarity differences across the membrane with and without the NKE pump. (c) Volume change with and without the NKE pump.

does not prescribe local electroneutrality off the space charge layers, but is naturally well satisfied in the model simulation.

D. Ionic current distributions and time courses. The time course of ionic currents (Na^+, K^+, Cl^-, and total) as well as ionic current distributions is shown in Figure 3. The time courses of transmembrane ionic currents and total current with and without NKE in Panel (a) and Panel (d). Ionic current distributions with and without NKE at t=5.0ms (panel (b) and panel (e)) and at t=19.2ms (c and f). Chemical potentials for sodium and potassium ionic species are also shown in red solid and dotted profiles.

With the free boundaries, the ionic current distributions are more complex. In case the boundaries are fixed, the sodium and potassium currents across the boundaries are solely outward and inward, respectively. On the other hand, when the boundaries are free, the sodium ionic currents are inward in the extracellular domain but outward in the intracellular domain. The case of potassium is more complicated. When the boundaries are free, the potassium ionic currents are inward in both of the extracellular and intracellular domains at t=5ms. However, the potassium ionic currents turn to be inward in the extracellular domain but outward in the intracellular domain at t=19.2ms. Chloride ionic currents are adjusted to satisfy the total current to be almost zero in the sense of electroneutrality.

When the active pump is turned off, sodium and potassium ionic currents are persistently inward and outward, respectively, i.e., passive permeation of those ionic species as the only transport across the membrane. Interestingly, the chloride ionic species has reverse flow in contrast to the case of working active pump, showing the involved pumping functionality implicitly without any explicitly prescribed active pumps in the way of total current to be almost zero in the sense of electroneutrality (Fig. S2 (f)).

E. vant Hoff's Law in the microscopic representation of the interaction between the membrane and dissolved solutes in fluid. Hydrostatic pressure profiles are shown in Figure S5. There is a dramatic change in hydrostatic pressure across the intracellular to extracellular domains. The hydrostatic pressure difference between the intracellular and extracellular domains is Δhydrostatic pressure, and the osmotic pressure difference between the intracellular and extracellular domains is Δosmotic pressure. Figure 4(a) and (b) show Δhydrostatic pressure versus Δosmotic pressure across the membranes as time courses of pressure and osmolarity differences with and without NKE. With active pumps working, Δhydrostatic pressure is less than Δosmotic pressure, and the difference is through the work done by active pumps. Without active pumps working, Δ hydrostatic pressure is approximately close to Δ osmotic pressure, and this is consistent with the macroscopic law of vant Hoff's Law:

$$(p_2 + K_{\mathrm{B}}T\sum_i c_{i,2}) - (p_1 + K_{\mathrm{B}}T\sum_i c_{i,1}) = RQ, \qquad [7]$$

where p_1 and $c_{i,1}$ are the extracullar hydrodynamic pressure and the concentration of ith ionic species, and p_2 and $c_{i,2}$ are the intracellular hydrodynamic pressure and the concentration of ith ionic species. All of them are out of the space charge layers. R is the water resistance and Q is the water flux from the intracellular to extracellular domains, which is zero in the 1D model. Active pumps are essentially necessary for volume regulation. As shown in Fig. 4(c), the volume is preserved due to the active pumps after transient adjustment in the beginning. On the other hand, the volume is immensely expanded to significant swelling when the active pump does not work.

F. Membrane thickness. The prescribed membrane thickness is around 300 nm. In the involved discretization of the numerical methods, refining the mesh and grids around the membrane will make the domain of the influence from the prescribed chemical potentials thinner, still in the non-asymptotic finite measure. Nevertheless, the competence of recapitulating physiological subcellular profiles of excitability in electrodiffusion is thought to be well conserved.

G. Generalizability for other types of active pumps. The proposed IB electrodiffusion active pump model focused on NKE is applicable to Na^+/H^+ and NKCC ($Na^+/K^+/2Cl^-$) cotransporters. One conjecture is that the asymmetry in the superposition of regularized singular integral and Heaviside kernels is sufficient for arbitrarily prescribed active transport

DRAFT

exchange currents in terms of intracellular and extracellular ionic concentrations and membrane voltage.

3. Conclusions

The newly developed IB electrodiffusion active pump model does reconstruct passive transport in the membranes via smoothed Dirac delta functions, and induced currents from active pumps via smoothed Heaviside kernels. This is a new model of active pumps in the presence of the space charge layers in the electrodiffusion. The free boundaries without an active pump show van't Hoff Law justifying the microscopic representation of fluctuation-dissipation from membrane to fluid and solutes/ions in the presence of chemical potentials. The model simulation reconstructs active pumping with volume preserved and swelling without active pumps while resolving the space charge layers in a non-asymptotic manner. An extension to 3D model simulations based on the IB electrodiffusion model of Poisson-Nernst-Planck equations coupled to Stokes flows remain for the future, where it will be intriguing to address the symmetry of Onsager's law from asymmetric chemical potentials. This is a foundation for applying the immersed boundary electrodiffusion active pump model for subcellular transport of water and molecules, possibly involving the cell motility and migration, such as dendritic spine motility and synaptic plasticity, and cellular migration, as well as cellular contraction, excitation-contraction coupling, and renal solute concentration.

Model and parameter optimization

The main numerical solvers of the partial differential equations and optimization is from the frameworks of PETSc (45).

A. Solving the electrodiffusion equations of the Poisson-Nernst-Planck coupled to free boundaries. For the spatial domain of 5μm, the spatial grids are 512 with $\Delta x = 9.766$nm. The time-stepping is $\Delta t = 3$ns. The main algorithmic flow is the following: 1) Apply Fast Fourier Transform (FFT) for solving the Poisson equation for the electrical potential. 2) Construct chemical potentials for each ionic species. 3) Incorporate a second-order Godunov-upwind method for reconstruction of concentration distributions for each ionic species. 4) Apply FFT for solving the hydrostatic pressure distributions. 5) Prescribe the advection of Lagrangian membrane coordinates of X_{a} and X_{b}.

B. Parametrization. For parameter optimization of chemical potentials, PETSc Tao framework with gradient-based optimization is incorporated.

ACKNOWLEDGMENTS. This article is expected to be a celebration of Charlie Peskin's 80th birthday. The author was partially supported by RCMI (U54MD013376) and ASCEND (UL1GM118973/ RL5GM118972) in the summer sabbatical research in Sean Sun's lab at Johns Hopkins.

1. Peskin C, Odell G, Oster G (1993) Cellular motions and thermal fluctuations: the brownian ratchet. *Biophysical Journal* 65:316–324.
2. Peskin C, Ermentrout B, Oster G (1994) *The correlation ratcher: a novel mechanism for generating directed motion by ATP hydrolysis*, ed. V.C. Mow ea. (Springer-Verlag, New York).
3. Oster G, Wang H (2003) Rotary protein motors. *TRENDS in Cell Biology* 13:114–121.
4. Sun S, Wang H, Oster G (2004) Asymmetry in the f1-atpase and its implications for the rotational cycle. *Biophysical Journal* 86:1373–1384.
5. Finkelstein A (1987) *Water Movement Through Lipid Bilayers, Pores, and Plasma Membranes : Theory and Reality*, Distinguished Lecture Series of the Society of General Physiologists. (Wiley, New York).
6. Spring K (1999) Epithelial fluid transport–a century of investigation. *News Physiol Sci* 14:92–98.
7. Su YC, Lin L, Pisano A (2002) A water-powered osmotic microactuator. *Journal of Microelectromechanical Systems* 11:6681–6692.
8. Evilevitch A, Lavelle L, Knobler C, Raspaud E, Gelbart W (2003) Osmotic pressure inhibition of dna ejection from phage. *Proc Natl Acad Sci USA* 100:9292–9295.
9. Zinemanas D, A.Nir (1995) Osmophoretic motion of deformable particles. *International Journal of Multiphase Flow* 21:787–800.
10. J. Nardi RB, Sackmann E (1999) Vesicles as osmotic motors. *Physical Review Letters* 82:5168–5171.
11. Dai J, Sheetz M, Wan X, Morris C (1998) Membrane tension in swelling and shrinking molluscan neurons. *J Neurosci* 18:6681–92.
12. O'Neill W (1999) Physiological signicance of volume-regulatory transporters. *American Journal of Physiology* 276:C995–C1011.
13. Baumgarten C (2006) Cell volume regulation in cardiac myocytes: a leaky boat gets a new bilge pump. *J Gen Physiol* 128:487–489.
14. Panayiotidis M, Bortner C, Cidlowski J (2006) On the mechanism of ionic regulation of apoptosis: would the na+/k+-atpase please stand up? *Acta Physiol (Oxf)* 187:205–215.
15. Stroka K, et al. (2014) Water permeation drives tumor cell migration in confined microenvironments. *Cell* 157:611–623.
16. Dukhin S (1993) Non-equilibrium electric surface phenomena. *Adv. Colloid Interface Sci.* 44:1–134.
17. Hayes M, Ewing A (1992) Electroosmotic flow control and monitoring with an applied radial voltage for capillary zone electrophoresis. *Anal Chem* 64:512–516.
18. Lee C, Blanchard W, Wu CT (1990) Direct control of the electroosmosis in capillary zone electrophoresis by using an external electric field. *Anal. Chem.* 62:1550– 1552.
19. Landers J (2003) Molecular diagnostics on electrophoretic microchips. *Anal. Chem.* 75:2919–2927.
20. Dolnik V, Hutterer K (2001) Capillary electrophoresis of proteins. *Electrophoresis* 22:4163–78.
21. Figeys D (2001) Proteomics on a chip : Promosing developments. *Electrophoresis* 22:208–216.
22. Lammert P, Prost J, Bruinsma R (1996) Ion drive for vesicles and cells. *J. Theor. Biol.* 178:387–391.
23. Fransaer J, Celis JP, Roos J (1991) Electro-osmophoresis of a charged permeable microcapsule with thin double layer. *J. Colloid Interface Sci.* 151:26–40.
24. Atzberger P, Kramer P (2007) Theoretical framework for microscopic osmotic phenomena. *Phys. Rev. E* 75:061125.
25. Atzberger P, Isaacson S, Peskin C (2009) A microfluidic pumping mechanism driven by non-equilibrium osmotic effects. *Physica D* 238:1168–1179.
26. Wu CH, Fai T, Atzberger P, Peskin C (2015) Simulation of osmotic swelling by the stochastic immersed boundary method. *SIAM J. Sci. Comput.* 37:B660–B688.
27. Lee P (2007) Ph.D. thesis (Courant Institute of Mathematical Sciences, New York University).
28. Lee P, Griffith B, Peskin C (2010) The immersed boundary method with advection-electrodiffusion with implicit timestepping and local mesh refinement. *Journal of Computational Physics* 229:5208–5227.
29. Lee P, Sobie E, Peskin C (2013) Computer simulation of voltage sensitive calcium ion channels in a dendritic spine. *Journal of Theoretical Biology* 11:87–93.
30. Peskin C (2002) The immersed boundary method. *Acta Num.* 11:479–517.
31. Finkelstein A (1964) Carrier model for active transport of ions across a mosaic membrane. *Biophysical Journal* 4:P421–440.
32. Bunow B (1978) Chemical reactions and membranes: a macroscopic basis for faciliated transport, chemiosmosis and active transport part i: Linear analysis. *J. Theor. Biol.* 75:51–78.
33. Endresen L, Hall K, Hoye J, Myrheim J (2000) A theory for the membrane potential of living cells. *European Biophysics Journal* 29:90–103.
34. Sala L, et al. (2019) A theoretical study of aqueous humor secretion based on a continuum model coupling electrochemical and fluid-dynamical transmembrane mechanisms. *Communications in Applied Mathematics and Computational Science* 14:65–102.
35. H J, SX S (2013) Cellular pressure and volume regulation and implications for cell mechanics. *Biophys J* 105:609–619.
36. J T, SX S (2015) Active biochemical regulation of cell volume and a simple model of cell tension response. *Biophys J* 109:1541–1550.
37. Yellin F, et al. (2018) Electromechanics and volume dynamics in nonexcitable tissue cells. *Biophys J* 114:2231–2242.
38. Chodhury M, et al. (2022) Kidney epithelial cells are active mechano-biological fluid pumps. *Nature Communications* 13:1–13.
39. Mori Y (2011) Mathematical properties of pump-leak models of cell volume control and electrolyte balance. *J. Math. Biol.* 65:875–918.
40. Jackle J (2017) The resting potential of nerve cells and the na,k-pump. arXiv:1703.03766.
41. Stinchcombe A, Mori Y, Peskin C (2015) Well-posed treatment of space-charge layers in the electroneutral limit of electrodiffusion. *Communications on Pure and Applied Mathematics* 69:2221–2249.
42. Banerjee T, et al. (2022) Spatiotemporal dynamics of membrane surface charge regulates cell polarity and migration. *Nature Cell Biology* 24:1499–1515.
43. Patel H, Barber D (2005) A developmentally regulated na-h exchanger in dictyostelium discoideum is necessary for cell polarity during chemotaxis. *Journal of Cell Biology*

DRAFT

169:321–329.
44. Green W, Andersen O (1991) Surface charges and ion channel function. *Annu. Rev. Physiol.* 53:341–359.
45. Balay S, Gropp W, McInnes L, Smith B (1997) Efficient management of parallelism in object oriented numerical software efficient management of parallelism in object oriented numerical software libraries in *Modern Software Tools in Scientific Computing*, eds. Arge E, Bruaset A, Langtangen H. (Birkhauser Press).

DRAFT